Quantum computation with Majorana zero modes in superconducting circuits

Heck, B. van

Author: Heck, Bernard van
Title: Quantum computation with Majorana modes in superconducting circuits
Issue Date: 2015-05-06

Chapter 2

Coulomb stability of the 4π-periodic Josephson effect of Majorana modes

The energy H_J of a tunnel junction between two superconductors (a Josephson junction) depends on the difference ϕ of the phase of the order parameter on the two sides of the junction. The derivative $I_J = (2e/\hbar)dH_J/d\phi$ gives the supercurrent flowing through the junction in the absence of an applied voltage. In a ring geometry, the supercurrent depends periodically on the flux Φ enclosed by the ring, with periodicity $h/2e$. This familiar DC Josephson effect [39, 40] acquires a new twist if the junction contains Majorana modes [26, 41, 42].

Majorana modes are charge-neutral quasiparticles bound to mid-gap states, at zero excitation energy, which appear in a so-called topologically non-trivial superconductor [43, 44]. While in the conventional Josephson effect only Cooper pairs can tunnel (with probability $\tau \ll 1$), Majorana modes enable the tunneling of single electrons (with a larger probability $\sqrt{\tau}$). The switch from $2e$ to e as the unit of transferred charge amounts to a doubling of the fundamental periodicity of the Josephson energy, from $H_J \propto \cos\phi$ to $H_J \propto \cos(\phi/2)$. In a ring geometry, the period of the flux dependence of the supercurrent I_J doubles from 2π to 4π as a function of the Aharonov-Bohm phase[1] $\varphi_0 = 2e\Phi/\hbar$. This 4π-periodic Josephson effect has been extensively studied theoretically [42, 45–50], as a way to detect the (so far, elusive) Majorana modes [51].

Since the Majorana modes in a typical experiment will be confined to superconducting islands of small capacitance C, the Coulomb energy $H_C = Q^2/2C$ associated with a charge difference $2Q$ across the junction competes with the Josephson energy.

[1]As a function of the enclosed flux, I_J has the same h/e periodicity as the persistent current I_N through a normal metal ring (radius R). One can distinguish the two currents by their size dependence: While I_N decays as $1/R$ or faster, I_J has the R-independence of a supercurrent.

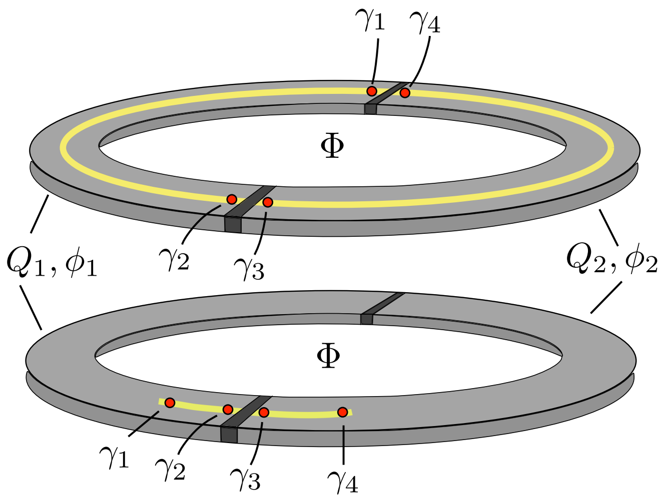

Figure 2.1: Geometry of a DC SQUID, consisting of a superconducting ring (grey) interrupted by two tunnel junctions (black) and threaded by a magnetic flux Φ. A semiconductor nanowire (yellow) contains Majorana modes at the end points (red dots). The two panels distinguish the cases that Majorana modes are present at both junctions (top), or only at a single junction (bottom). The 4π-periodic Josephson effect is stable against quantum phase slips in the first case, but not in the second case.

The commutator $[\phi, Q] = 2ei$ implies an uncertainty relation between charge and phase differences, so that a nonzero H_C introduces quantum fluctuations of ϕ in the ground state [40]. What is the fate of the 4π-periodic Josephson effect?

As we will show in this chapter, the supercurrent through the ring remains a 4π-periodic function of φ_0, regardless of the relative magnitude of H_C and H_J. This Coulomb stability requires that all weak links in the ring contain Majorana modes. If the ring has a topologically trivial segment, then quantum phase slips restore the conventional 2π-periodicity of the Josephson effect on sufficiently long time scales. We calculate the limiting time scale for the destruction of the 4π-periodic Josephson effect by quantum phase slips and find that it can be much shorter than the competing time scale for the destruction of the 4π-periodicity by quasiparticle poisoning [42].

2.1 Hamiltonian of a DC SQUID with Majorana modes

We apply the general theory of Majorana-Josephson junction arrays of Xu and Fu [52] to the DC SQUID geometry of Fig. 2.1, consisting of two superconducting islands separated by tunnel junctions. The islands have a charge difference $2Q = Q_1 - Q_2$, with $Q_n = -2ei\partial/\partial\phi_n$ canonically conjugate to the superconducting phase ϕ_n. The gauge invariant phase differences across the two junctions are given by $\phi = \phi_1 - \phi_2$ and $\varphi_0 - \phi$. Here we assume that the ring is sufficiently small that the flux generated by the supercurrent can be neglected, so the enclosed flux equals the externally applied flux[2].

Each island contains a segment of a semiconductor nanowire, driven into a topologically nontrivial superconducting state by the proximity effect [45, 46] (alternatively, the nanowire could be replaced by the conducting edge of a two-dimensional topological insulator [42]). The Majorana modes appearing at the end points of each segment are represented by anti-commuting Hermitian operators $\gamma_1, \gamma_2, \gamma_3, \gamma_4$ that square to unity,

$$\gamma_n = \gamma_n^\dagger, \;\; \gamma_n\gamma_m + \gamma_m\gamma_n = 2\delta_{nm}. \tag{2.1}$$

The Majorana modes are coupled by the tunnel junction. We distinguish two cases. In the first case (top panel in Fig. 2.1) each of the two tunnel junctions couples a pair of Majorana modes. In the second case (bottom panel) one pair of Majorana modes is coupled by a Josephson junction, while the other pair remains isolated.

The Hamiltonian $H = H_C + H_{J,1} + H_{J,2}$ is the sum of charging and Josephson energies,

$$H_C = \frac{1}{2C}(Q + q_{\rm ind})^2, \tag{2.2}$$

$$H_{J,1} = E_{M,1}\Gamma_1 \cos\frac{\phi}{2} - E_{J,1}\cos\phi, \tag{2.3}$$

$$H_{J,2} = E_{M,2}\Gamma_2 \cos\frac{\varphi_0 - \phi}{2} - E_{J,2}\cos(\varphi_0 - \phi), \tag{2.4}$$

$$\Gamma_1 = i\gamma_2\gamma_3, \;\; \Gamma_2 = i\gamma_4\gamma_1. \tag{2.5}$$

The induced charge $q_{\rm ind} = C_g V_g$ accounts for charges on nearby electrodes, controlled by a gate capacitance C_g and gate voltage V_g. The energy scales $E_{M,n}$ and $E_{J,n}$ quantify the Josephson coupling strength of, respectively, single electrons and electron pairs. With this Hamiltonian we can describe both cases considered, by putting $E_{M,2} = 0$ for the junction without Majorana modes.

The eigenstates $\Psi(\phi_1, \phi_2)$ of H should satisfy the fermion parity constraint [36]

$$\Psi(\phi_1 + 2\pi n, \phi_2 + 2\pi m) = (-1)^{nq_1}(-1)^{mq_2}\Psi(\phi_1, \phi_2), \tag{2.6}$$

$$q_n = \tfrac{1}{2}(1 - p_n), \;\; p_1 = i\gamma_1\gamma_2, \;\; p_2 = i\gamma_3\gamma_4. \tag{2.7}$$

The operators q_n and p_n have, respectively, eigenvalues $0, 1$ and ± 1, depending on whether island n contains an even or an odd number of electrons. The constraint (2.6) enforces that the eigenvalues of Q_n are even multiples of e for $q_n = 0, p_n = 1$ and odd multiples of e for $q_n = 1, p_n = -1$.

[2] The flux induced by the supercurrent I_J due to the nonzero inductance $L \simeq \mu_0 R$ of the ring may be neglected relative to the applied flux if $LI_J \ll \hbar/e$. The magnitude of the supercurrent can be estimated by $\hbar I_J/e \simeq \min(E_J, E_J^2/E_C) \equiv E_c$. For $E_c \simeq 1\,$meV the induced flux can be neglected if $R \ll 1\,$cm.

It is possible to solve the eigenvalue problem $H\Psi = E\Psi$ subject to the constraint (2.6), along the lines of Ref. [52], but alternatively one can work in an unrestricted Hilbert space. The restriction is removed by the unitary transformation

$$\Psi = U_1 U_2 \tilde{\Psi}, \;\; U_n = \exp(i q_n \phi_n/2). \tag{2.8}$$

The function $\tilde{\Psi}(\phi_1, \phi_2)$ is 2π-periodic in each of its arguments, so the constraint (2.6) is automatically satisfied. Now the eigenvalues of Q_n are all even multiples of e. The transformed Hamiltonian $\tilde{H} = (U_1 U_2)^\dagger H U_1 U_2$ becomes

$$\begin{aligned}\tilde{H} = {} & \frac{1}{2C}\Big(Q + \frac{eq_1 - eq_2}{2} + q_{\rm ind}\Big)^2 \\ & + \tfrac{1}{2}\big[e^{-iq_1\phi_1}\big(E_{M,1}\Gamma_1 + E_{M,2}\Gamma_2 e^{i\varphi_0/2}\big)e^{iq_2\phi_2} + \text{H.c.}\big] \\ & - E_{J,1}\cos\phi - E_{J,2}\cos(\varphi_0 - \phi),\end{aligned} \tag{2.9}$$

where we have used the identity

$$U_n^\dagger \Gamma_m e^{i\phi_n/2} = \Gamma_m U_n. \tag{2.10}$$

Notice that the Hamiltonian has become 2π-periodic in the superconducting phases ϕ_1, ϕ_2, while remaining 4π-periodic in the flux φ_0. Notice also that $\tilde{H}$ may depend on the ϕ_n's separately, not just on their difference. This does not violate charge conservation, because the conjugate variables Q_n now count only the number of Cooper pairs on each island — not the total number of electrons.

The four Majorana modes encode a qubit degree of freedom [6]. The states of the qubit are distinguished by the parity of the number of electrons on each island. If the total number of electrons in the system is even ($\mathscr{P} = 1$), the qubit states are $|11\rangle$ and $|00\rangle$, while for an odd total number of electrons ($\mathscr{P} = -1$) the states are $|10\rangle$ and $|01\rangle$. In this qubit basis, the products of Majorana operators appearing in the Hamiltonian (2.9) are represented by Pauli matrices,

$$q_1 = \tfrac{1}{2} + \tfrac{1}{2}\sigma_z, \;\; q_2 = \tfrac{1}{2} + \tfrac{1}{2}\mathscr{P}\sigma_z, \;\; \Gamma_1 = -\sigma_x, \;\; \Gamma_2 = \mathscr{P}\sigma_x. \tag{2.11}$$

It is straightforward to calculate the eigenvalues of $\tilde{H}$, by evaluating its matrix elements in the basis of eigenstates of Q. The spectrum $E_n^{\mathscr{P}}(\varphi_0, q_{\rm ind})$ as a function of the enclosed flux and the induced charge has two branches distinguished by the total fermion parity $\mathscr{P} = \pm 1$, with

$$E_n^+(\varphi_0, q_{\rm ind}) = E_n^-(\varphi_0 + 2\pi, q_{\rm ind} + e/2). \tag{2.12}$$

2.2 DC SQUID with two Majorana junctions

We first consider the case that both junctions contain Majorana modes (top panel in Fig. 2.1). A fully analytical calculation is possible in the limit that the charging energy dominates over the Josephson energy ($E_C \equiv e^2/2C \gg E_{M,n}, E_{J,n}$). Only the

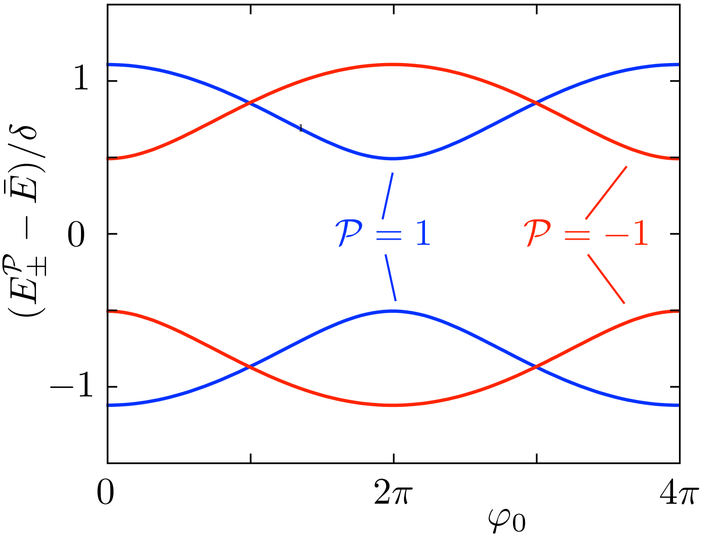

Figure 2.2: Spectrum of the DC SQUID in the top panel of Fig. 2.1, containing Majorana modes at both Josephson junctions. The curves are the result (2.13), in the limit that the charging energy dominates over the Josephson energy. The parameters chosen are $E_{M,1} = E_{M,2} = \delta$. The level crossing is between states of different fermion parity $\mathscr{P}$, and therefore there can be no tunnel splitting due to the Coulomb interaction (which conserves $\mathscr{P}$).

two eigenstates of Q with lowest charging energy $\bar{E} \pm \frac{1}{2}\delta$ are needed in this limit and $2e$ tunnel processes may be neglected relative to e tunnel processes (so we may set $E_{J,n} = 0$). We thus obtain the simple expression

$$E_\pm^{\mathscr{P}} = \bar{E} \pm \tfrac{1}{2}\left[\delta^2 + E_{M,1}^2 + E_{M,2}^2 + 2\mathscr{P} E_{M,1}E_{M,2}\cos\frac{\varphi_0}{2}\right]^{1/2}. \tag{2.13}$$

The resulting 4π-periodic spectrum is shown in Fig. 2.2.

The crossing of the two branches E_-^+ and E_-^- at $\varphi_0 = \pi$ is protected, regardless of the value of E_C, because the charging energy cannot couple states of different $\mathscr{P}$. Quasiparticle poisoning (the injection of unpaired electrons) switches the fermion parity on a time scale T_p, which means that the 4π-periodicity of the energy of the ring can be observed if the enclosed flux is increased by a flux quantum in a time $T_\Phi \ll T_p$.

2.3 DC SQUID with a single Majorana junction

We now turn to the case that one of the two Josephson junctions does not contain Majorana modes (lower panel in Fig. 2.1). By putting $E_{M,2} = 0$ the Hamiltonian

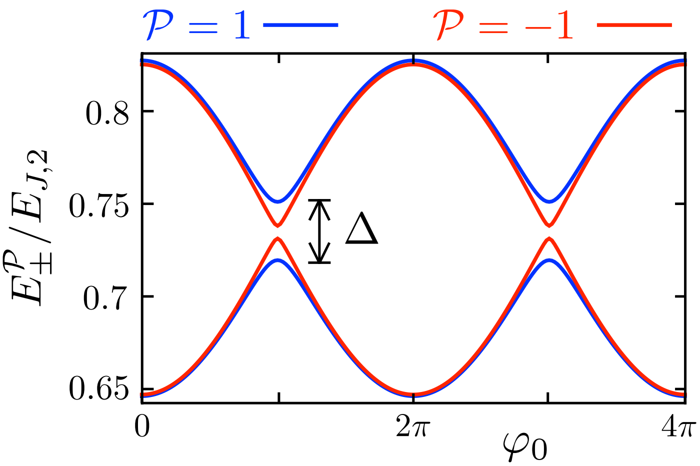

Figure 2.3: Spectrum of the DC SQUID in the bottom panel of Fig. 2.1, containing Majorana modes at only one of the two Josephson junctions. The curves are a numerical calculation for the full Hamiltonian, in the regime that the Josephson energy of the trivial junction is the largest energy scale. The parameters chosen are $E_{J,2}=4E_C=10E_{M,1}$, $E_{M,2}=0=E_{J,1}$, and $q_{\rm ind}=0$. In contrast to Fig. 2.2, a tunnel splitting Δ appears because the level crossing is between states of *the same* fermion parity.

becomes 2π-periodic in φ_0. In Fig. 2.3 we show the spectrum for a relatively large Josephson energy of the trivial junction. The phase ϕ is then a nearly classical variable, which in the ground state is close to φ_0 (mod 2π). The charging energy opens a gap in the spectrum near $\varphi_0=\pi$ (mod 2π), by inducing tunnel processes from $\phi=\varphi_0$ to $\phi=\varphi_0\pm 2\pi$ (quantum phase slips). A tunnel splitting by the $\mathscr{P}$-conserving charging energy is now allowed because the level crossing is between states of the same $\mathscr{P}$.

A semiclassical calculation of the tunnel splitting due to quantum phase slips at the trivial Josephson junction, along the lines of Ref. [37], gives for $E_J\equiv E_{J,2}\gg E_C\gg E_{M,1}\equiv E_M$ the spectrum

$$E_{\pm}^{\mathscr{P}}=-E_J+\sqrt{2E_CE_J}\pm\sqrt{E_M^2\cos^2(\varphi_0/2)+\Delta^2}, \tag{2.14}$$

$$\Delta=16\big(E_CE_J^3/2\pi^2\big)^{1/4}\exp\big(-\sqrt{8E_J/E_C}\big)\times \times\sqrt{\cos^2(\pi q'_{\rm ind}/e)+\frac{\pi^2E_M^2}{8E_CE_J}\sin^2(\pi q'_{\rm ind}/e)}, \tag{2.15}$$

where we have abbreviated $q'_{\rm ind}=q_{\rm ind}+(e/4)(1-\mathscr{P})$. The second term on the right-hand-side of Eq. (2.14) describes the effect of zero-point fluctuations of ϕ around the values φ_0 and $\varphi_0\pm 2\pi$. Tunnel processes $\phi=\varphi_0\mapsto\varphi_0+2\pi$ and $\phi=\varphi_0\mapsto\varphi_0-2\pi$ produce the third term. The sine and cosine factors in Eq. (2.15) accounts for

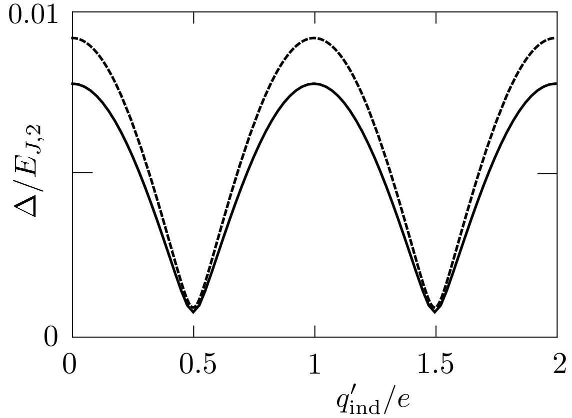

Figure 2.4: Tunnel splitting at $\varphi_0 = \pi$ as a function of the induced charge. The dashed curve correspond to Eq. (2.15), the solid curve to numerical calculations for the full Hamiltonian, for $E_{J,2} = 5\,E_C = 25\,E_{M,1}$ (with $E_{M,2} = 0 = E_{J,1}$).

interference between these two quantum phase slip processes (Aharonov-Casher effect) [35, 53–56] .The numerical calculation in Fig. 2.4 agrees quite well with the semiclassical approximation (2.15).

The tunnel splitting Δ ensures that the energy of the ring evolves 2π-periodically if the flux Φ is increased by a flux quantum $h/2e$ in a time T_Φ which is long compared to $T_\Delta = \hbar E_{M,1}/\Delta^2$. For $T_\Phi \lesssim T_\Delta$ there is a significant probability $\exp(-T_\Phi/T_\Delta)$ for a Landau-Zener transition through the gap, resulting in a 4π-periodic evolution of the energy.

This limiting time scale T_Δ originating from quantum phase slips can be compared with the time scale T_p for quasiparticle poisoning. We require T_Φ small compared to both T_Δ and T_p to observe the 4π-periodic Josephson effect. For $\Delta > (\hbar E_{M,1}/T_p)^{1/2}$ one has $T_\Delta < T_p$, so quantum phase slips govern. A recent experiment finds $T_p \simeq 2\,\text{ms}$ in Al for temperatures below 160 mK [57]. Since $E_{M,1}$ will be well below 1 meV, one has $T_\Delta < T_p$ if quantum phase slips occur with a rate $\Delta/\hbar$ higher than 30 MHz. While quantum phase slip rates can vary over many orders of magnitude due to the exponent in Eq. (2.15), typical values for a DC SQUID are in the GHz range.

In conclusion, we have shown that Coulomb charging effects do not spoil the 4π-periodic Josephson effect in a superconducting ring, provided that all weak links contain Majorana modes. Quantum phase slips at a weak link without Majorana modes restore the 2π-periodicity on time scales long compared to a time T_Δ, which may well be shorter than the time scale for quasiparticle poisoning.

The origin of the protection of the 4π periodicity if the entire ring is topologically nontrivial is conservation of fermion parity [42] (See Ref. [58] for a more general perspective.) This protection breaks down if part of the ring is a trivial superconductor, because then the level crossing involves states of the same fermion parity and tunnel splitting by the charging energy is allowed (see Fig. 2.3).

We note in closing that the different stability of the 4π-periodic Josephson effect in the two geometries of Fig. 2.1, examined here with respect to Coulomb charging, extends to other parity-preserving perturbations of the Hamiltonian. For example, overlap of the wave functions of two Majorana bound states on the same island introduces a term $H_{\text{overlap}} = i\epsilon\gamma_1\gamma_2$. For the lower panel of Fig. 2.1, this term leads to a tunnel splitting $\Delta = 2\epsilon$ which spoils the 4π-periodicity [26]. For the upper panel of Fig. 2.1, $\Delta \equiv 0$ because H_{overlap} preserves fermion parity.